

# RSC Advances



This is an *Accepted Manuscript*, which has been through the Royal Society of Chemistry peer review process and has been accepted for publication.

*Accepted Manuscripts* are published online shortly after acceptance, before technical editing, formatting and proof reading. Using this free service, authors can make their results available to the community, in citable form, before we publish the edited article. This *Accepted Manuscript* will be replaced by the edited, formatted and paginated article as soon as this is available.

You can find more information about *Accepted Manuscripts* in the [Information for Authors](#).

Please note that technical editing may introduce minor changes to the text and/or graphics, which may alter content. The journal's standard [Terms & Conditions](#) and the [Ethical guidelines](#) still apply. In no event shall the Royal Society of Chemistry be held responsible for any errors or omissions in this *Accepted Manuscript* or any consequences arising from the use of any information it contains.

## ARTICLE

Cite this: DOI:  
10.1039/x0xx00000x

Received 00th January 2012,  
Accepted 00th January 2012

DOI: 10.1039/x0xx00000x

www.rsc.org/

## Fabrication of a dye-sensitized solar cell module using spray pyrolysis deposition of a TiO<sub>2</sub> colloid

T. G. Deepak<sup>a</sup>, G. S. Anjusree<sup>a</sup>, K. R. Narendra Pai<sup>a</sup>, Devika Subash<sup>a</sup>, Shantikumar V Nair<sup>a</sup> and A. Sreekumaran Nair<sup>\*a</sup>

We provide a complete illustration of dye-sensitized solar module fabrication by spray pyrolysis deposition (SPD) of a TiO<sub>2</sub> colloid having ~ 10 nm size TiO<sub>2</sub> nanoparticles. The process was first optimized for cell level fabrication and the parameters (mainly the thickness) obtained from the study were subsequently used for module level fabrication. The best efficiency obtained in cell level (area 0.2 cm<sup>2</sup> and thickness of 12 μm) was 7.79 % and that for the (12 cm × 12 cm) module was 3.2%.

### Introduction

The solar energy would play an important role to satisfy the energy needs of mankind since coal and natural reserves are being consumed at faster rates.<sup>1</sup> The processing and manufacturing costs of widely used Si solar panels are high.<sup>2,3</sup> Further innovations in material science and technology are needed to make solar energy affordable to common man. The dye-sensitized solar cells (DSCs) developed by Grätzel and O'Regan using nanocrystalline semiconductor oxide material sensitized by a ruthenium (Ru) dye made a paradigm shift in field of solar energy conversion technology.<sup>4</sup> This pioneering work provided a new outlook to solar energy conversion technology which integrated different fields of science. Best efficiency achieved for DSCs has been 12% by using conventional Ru dye and liquid electrolyte system. Recently, a record power efficiency of 15% was obtained at cell level for perovskite-sensitized solar cell using Cobalt (π/III)-based electrolyte.<sup>5</sup> DSC solar panels are potential candidates for indoor lighting purposes because they slightly outperform the conventional Si solar panels under low Sun illuminations.<sup>6,7</sup> Simple fabrication methods at low temperatures make DSCs appealing over Si solar cells in solar energy market.

Doctor-blading is the widely used technique for thin film fabrication on transparent conductive oxide (TCO) substrate at

R&D level.<sup>8</sup> But it has major demerits like: 1) doctor-blading is not a scalable method, and 2) lack of reproducibility on the thickness and uniformity of the thin film. In this work, we have adopted a scalable *spray pyrolysis deposition (SPD)* technique

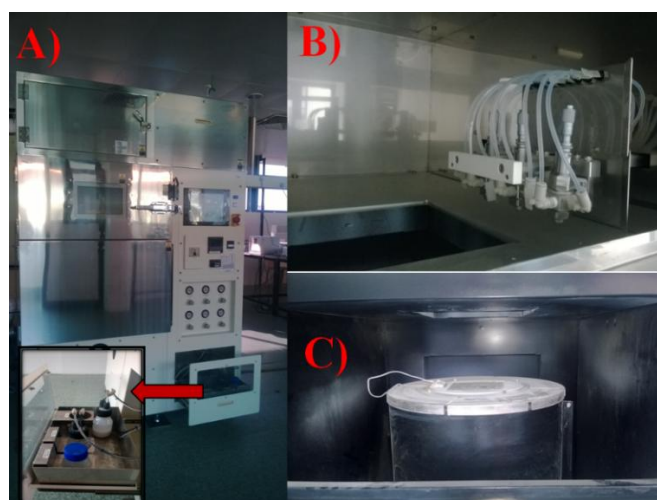


**Fig. 1.** A) An overview of the spray pyrolysis deposition machine (KM-150). Inset shows the chamber where solution for spraying is loaded. B) Three nozzles of the machine by which flow-rate of solution can be controlled for controlled deposition. C) A high temperature furnace inside the machine by which glass substrate can be pre-heated for thin film deposition.

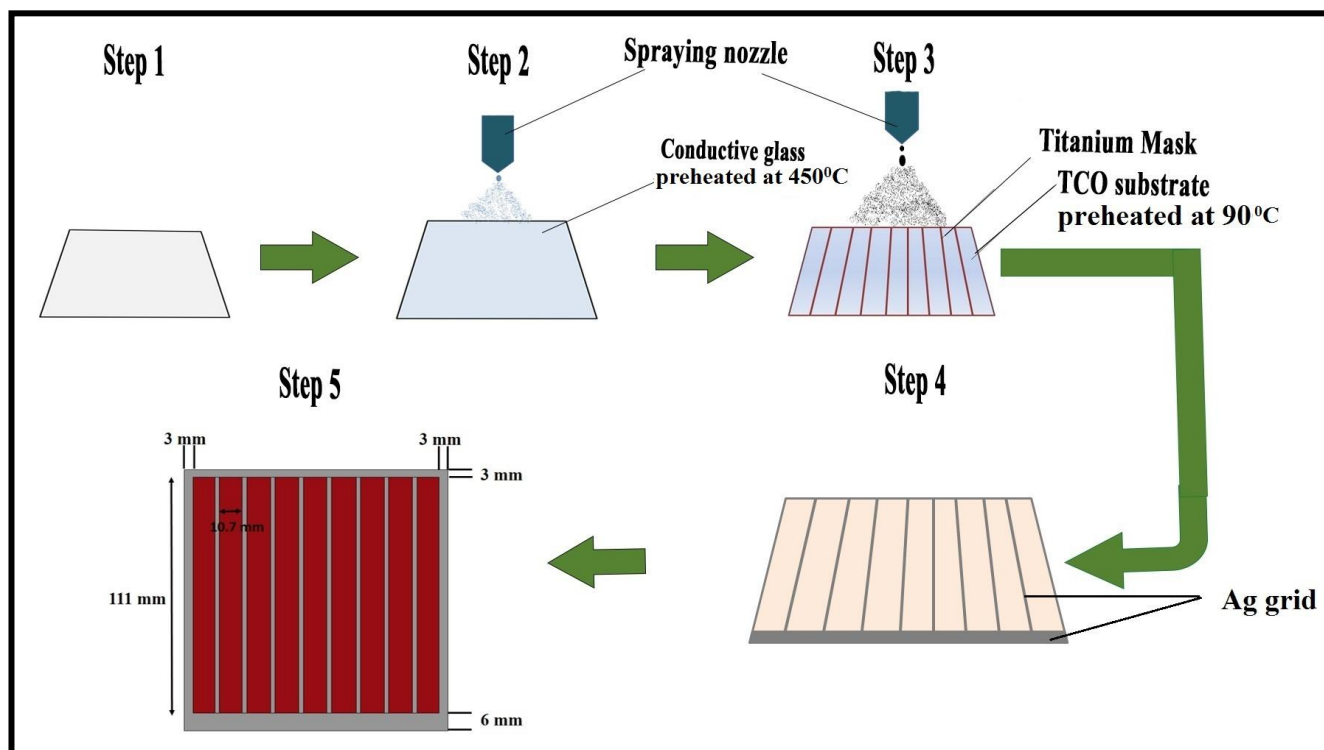


**Fig. 2.** Schematic showing the different steps of fabrication of dye-sensitized solar cell module. In Step 1: Corning Eagle XG plane glass with  $\sim 100\%$  transparency is heated at  $450\text{ }^{\circ}\text{C}$ . Step 2: Precursors of FTO are sprayed onto the glass plate to make it transparent conductive oxide substrate where transparency of glass is almost retained. Step 3:  $\text{TiO}_2$  colloidal solution is sprayed at  $90\text{ }^{\circ}\text{C}$  on masked FTO (masking is done by a metal grid as shown in Fig. 4) for  $12\text{ }\mu\text{m}$  thickness. Step 4: Ag grid was drawn on unmasked areas of FTO and sintered at  $530\text{ }^{\circ}\text{C}$  for 1 h. Step 5:  $\text{TiO}_2$  film was sensitized with N719 dye in a dye coating bath for 20 h.

using an automated machine (SPD Laboratory Inc., Japan) where the thickness of the film can be easily and accurately controlled. The optimized  $\text{TiO}_2$  film thickness is essential for reproducible efficiency since it controls both the dye loading and the extent of electron transport before collection. Generally in cell fabrication,  $10\text{ }\mu\text{m}$  has been adopted in view of efficient charge collection.<sup>9</sup> In the present case, we have used optimized thickness of film by spray pyrolysis deposition at cell level and the same thickness has been adopted for module fabrication using spray pyrolysis deposition.

### Experimental Methods

For DSCs fabrication, one side of the glass substrate (Corning Eagle XG, USA) was made conductive by spray pyrolysis deposition of fluorine and tin oxide precursors using a spray pyrolysis deposition machine (KM-150, SPD Laboratory, Inc. Japan). **Fig. 1** shows important parts of the SPD machine, KM-150. Dibutyltin diacetate (DBTDA) in 2-Propanol (0.2 M) and Ammonium fluoride ( $\text{NH}_4\text{F}$ ) in water (9 M) were mixed and stirred for making the precursors of the FTO.<sup>10</sup> By controlling the number of spraying cycles, an optimum thickness of 800 nm was deposited on glass substrate. The sheet resistance of the FTO plates was  $\sim 8\text{-}10\text{ }\Omega/\square$ .

The  $\text{TiO}_2$  colloidal solution for spraying was prepared as follows: A 2.5 mL of acetic acid (NICE Chemicals, India) and

20 mL of titanium isopropoxide (Sigma Aldrich, 99.9%) were added in 25 mL isopropyl alcohol (IPA, Sigma Aldrich, 99.9%). To obtain a  $\text{TiO}_2$  colloidal solution, steam was passed through the prepared solution which resulted in the expulsion of IPA and precipitation of the  $\text{TiO}_2$  colloidal mass. Then the  $\text{TiO}_2$  colloidal mass was grounded in a mortar with 50 mL water and autoclaved at  $180\text{ }^{\circ}\text{C}$  for 3h. The  $\text{TiO}_2$  film was deposited on FTO plates by spray pyrolysis deposition method using the KM-150 machine. The  $2 \times 2\text{ cm}^2$   $\text{TiO}_2$  films with different thicknesses were fabricated on FTO plates by varying the number of spraying cycles in the KM-150 machine. Thickness of the film was varied between  $6\text{ }\mu\text{m}$  to  $18\text{ }\mu\text{m}$  for optimizing

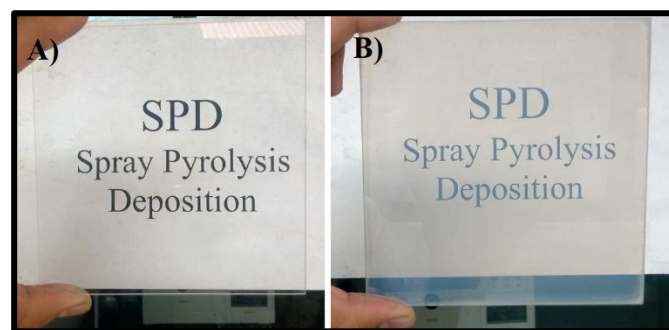


**Fig. 3.** A) The  $12 \times 12\text{ cm}^2$  Corning glass (bare) substrate. B) shows the transparency of the FTO-coated glass.



**Fig. 4.** The metallic (Ti) mask used to spray-deposit  $\text{TiO}_2$  as compartments on the FTO substrate.

the desired thickness for the  $\text{TiO}_2$  film. The films were sintered at  $450\text{ }^\circ\text{C}$  for 30 min. After sintering, an active area of  $0.2\text{ cm}^2$  was carved out from the film for dye deposition. The  $\text{TiO}_2$  films were soaked in 3 mM solution of the dye (N719) in acetonitrile and tert-butyl alcohol (1:1) for 12 h. The photoanode and counter electrode were sealed together with a UV sealant and filled with iodide/triiodide ( $\text{I}^-/\text{I}_3^-$ ) electrolyte by a vacuum back-filling process. The current density-voltage ( $J$ - $V$ ) characteristics of DSCs were measured using a Keithley 2400 source meter (Newport Oriel class A-Solar simulator, USA). The internal quantum efficiency of the DSCs was measured as a function of wavelength using an IPCE measurement instrument (Oriel Newport (QE-PV-SI/QE) IPCE Measurement kit, USA). A 230 W xenon (Oriel) lamp was used as light source for generating monochromatic light. The  $J$ - $V$  characteristics of dye solar module were measured using large area solar simulator (XES - 200S1, SAN-EI Electric, Japan). The intelligent design and precise fabrication technique adopted for dye solar module are shown in **Fig. 2** that make sure the maximal usage of FTO as active area. The large area  $12 \times 12\text{ cm}^2$  dye solar module was fabricated by employing the optimized  $\text{TiO}_2$  film thickness. The KM-150 machine was used for depositing FTO on the  $12 \times 12\text{ cm}^2$  glass substrate as documented in the schematic above. The transparency of FTO glass substrate is evident from **Fig. 3**. Subsequently the  $\text{TiO}_2$  colloidal solution was sprayed on the pre-heated (at  $90\text{ }^\circ\text{C}$ ) FTO glass substrate. The FTO was partially masked during the spraying of  $\text{TiO}_2$  colloidal solution using a metallic mask (**Fig. 4**). This masking also facilitated to draw silver (Ag) grid lines through the masked areas for charge collection. The  $\text{TiO}_2$  got deposited on the FTO glass substrate on unmasked regions. The  $\text{TiO}_2$  deposition resulted in rectangular-shaped cells or compartments in parallel. The silver grid was drawn on unmasked regions using an Ag grid drawing robot (SPD Laboratory, Inc. Japan) for proper electron collection to the external circuit. The  $\text{TiO}_2$ -coated FTO glass was sintered at  $530\text{ }^\circ\text{C}$  for 1 h. Then it was mounted in a dye coating bath machine which provided temperature controlled

dye-sensitization of the  $\text{TiO}_2$  film. The temperature was set at  $26\text{ }^\circ\text{C}$ . The washing of DSC by acetonitrile and drying were also carried out by the dye coating bath machine. The holes were drilled on Pt-coated glass substrate by a hole-drilling robot to fill the electrolyte through a vacuum back-filling process. The UV curable sealant was drawn on the Ag grid pattern which acted both as sealant and protective cover for the Ag (since  $\text{I}^-/\text{I}_3^-$  electrolyte is corrosive, that can react with the Ag grid lines).

The dye-sensitized photoanode and the hole-drilled counter electrode were sandwiched using an electrode pile-up machine (SPD Laboratory Inc., Japan). This was further exposed to UV irradiation for hardening of the sealant. Electrolyte was filled through the holes in the counter electrode using the vacuum back-filling process. After electrolyte filling, the holes were sealed by a glass slide using the UV sealant.

The  $\text{TiO}_2$  colloid used for spraying was characterized by transmission electron microscopy (TEM). The sample solution was drop-casted on carbon-coated copper grid and dried for TEM analysis. Powder XRD was carried out by X'pert pro PAN Analytical with a data interval of  $0.03^\circ$ , at current and voltage of 30 mA and 40 KV, respectively. The XPS (Kratos Analytical, UK) was used for elemental characterization of the material and for assessing the oxidation state of the elements involved. The carbon correction was done using the standard software from the manufacturer.

## Results and Discussion

### Characterization of the $\text{TiO}_2$ colloidal solution

**Fig. 5A** shows powder XRD pattern of the  $\text{TiO}_2$  used for spraying which indicates its anatase nature and crystallinity. The major peaks are indexed in the spectrum itself (JCPDS file no. 21-1272). The particle size estimated using Debye-Scherrer equation [from the full width-half maximum of the (101) peak] was  $\sim 12\text{ nm}$ . This was further supported by the TEM studies (**Fig. 6A** and **6C**, respectively).

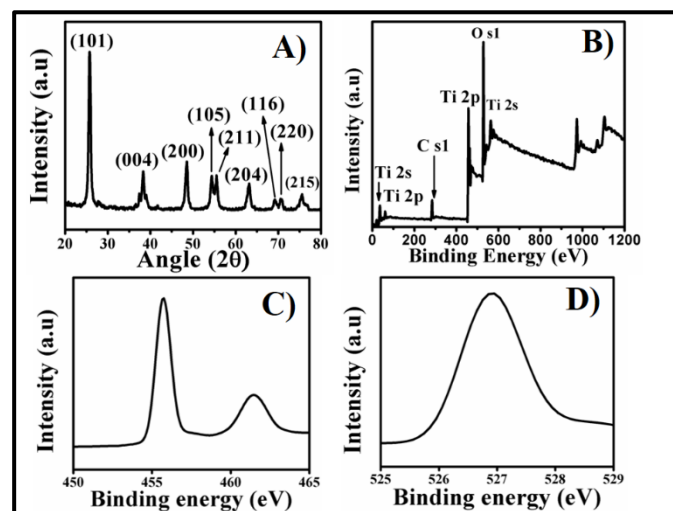


**Fig. 5.** A) Powder XRD spectrum and B) wide XPS spectrum of the  $\text{TiO}_2$  in the  $\text{TiO}_2$  colloidal solution. C & D show the high-resolution XPS spectra of C) Ti and D) O, respectively.



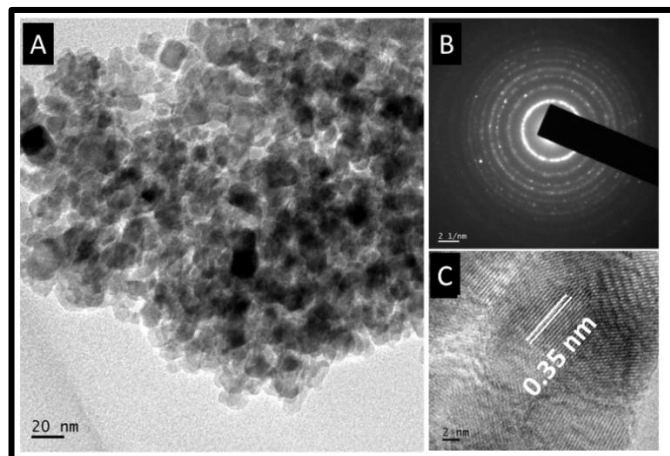


**Fig. 6.** A) TEM image showing the morphology of the TiO<sub>2</sub> in the colloidal solution B) its SAED pattern showing polycrystallinity and C) HRTEM image showing the 0.35 nm lattice spacing corresponding to the anatase TiO<sub>2</sub>.

TEM image indicated nearly monodisperse spherical particles of average diameter of 10 nm. The selected-area electron diffraction (SAED) pattern shown in **Fig. 6B** further confirms the polycrystalline nature of the TiO<sub>2</sub>. **Fig. 5C** shows a lattice-resolved image showing the most prominent (101) lattice orientation with a spacing of 0.35 nm.

XPS was used to determine the elemental composition and oxidation state of the TiO<sub>2</sub>. The **Fig. 5B** shows wide scan spectrum which gives elemental composition (Ti and O) of the material. The peaks at binding energies 455.71 eV and 461.48 eV correspond to that of Ti 2p<sub>3/2</sub> and Ti 2p<sub>1/2</sub>, respectively (**Fig. 5C**). The O1s showed a single peak at 526.90 eV (**Fig. 5D**).<sup>11</sup>

### Photovoltaic (PV) performance of DSCs

Since TiO<sub>2</sub> film has lower electron drift mobility (10<sup>-4</sup>-10<sup>-7</sup> cm<sup>2</sup>/Vs), optimization of film thickness was inevitable in fabricating efficient dye-sensitized solar cell modules. At cell level, different TiO<sub>2</sub> thickness (10 μm, 12 μm, 15 μm, respectively) were fabricated and the PV parameters have been

**Table 1.** Variations of  $V_{oc}$ , current density, fill factor, IPCE (%) and efficiency with respect to change in thickness of the film.

Thickness of the film	$V_{oc}$ (V)	Current density (mA cm <sup>-2</sup> )	Fill factor (%)	Efficiency (%)
10 μm	0.759	11.94	73.88	6.70
12 μm	0.755	13.94	74	7.79
15 μm	0.75	13.86	73.18	7.61
18 μm	0.67	10.70	66.40	4.78

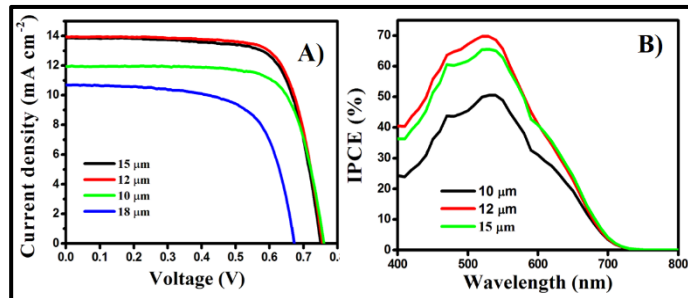


**Fig. 7.** A) Current density-Voltage ( $J$ - $V$ ) characteristics B) IPCE (%) of DSCs with different TiO<sub>2</sub> film thicknesses.

compared to obtain the optimum thickness for best performance. It was found that 12 μm thick TiO<sub>2</sub> film gives the best overall efficiency at cell level. The  $J$ - $V$  performance of cells with different TiO<sub>2</sub> thickness is shown in **Fig. 7 A**. An overall efficiency of 7.79% was obtained for the 12 μm thick TiO<sub>2</sub> film. The high  $V_{oc}$  (0.75 V) and current density (13.94 mA cm<sup>-2</sup>) make the 12 μm thick film a better performing DSC compared to those from the other TiO<sub>2</sub> films.

As TiO<sub>2</sub> thickness was increased, the internal resistance of the cell increased considerably and this contributed to a decrease in FF (**Fig. 8a**). The IPCE (%) of 70.5 % has been obtained for the 12 μm thick TiO<sub>2</sub> film (**Fig. 7B**). It shows the spectral response of current flown to the external circuit, where highest current was shown at the wavelength 525 nm which corresponds to the absorption maximum of the dye. Lower dye loading at thinner films and poor electron collection at thicker films contribute to a lower  $J_{sc}$  above and below the optimum film thickness. The  $V_{oc}$  was almost stable at lower thicknesses, but as thickness is increased, the same lowered considerably.

The increase in film thickness increases the number of trapping surface states and enhances the back electron transfer to the I<sub>3</sub><sup>-</sup> which would eventually result in lowering of  $V_{oc}$  and  $J_{sc}$ . The increase in thickness would increase the resistance of the cell; this could reduce the power loss in the system (i.e. lowering of FF). Electrochemical Impedance Spectroscopy (EIS) was used for confirming film thickness dependence on interfacial charge recombination.<sup>12</sup> The impedance measurements were carried out by applying a bias voltage equal to open-circuit voltage ( $V_{oc}$ ) at dark. The frequency varied from

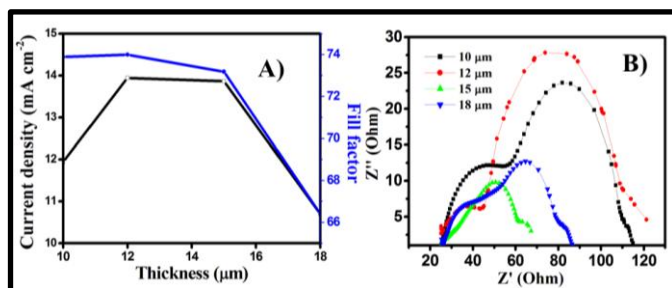


**Fig. 8.** A) The plot showing the dependence of current density and fill factor on film thickness. B) Nyquist plots obtained from EIS showing interfacial recombination resistance of different DSCs with different film thicknesses (for a proper comparison, all the impedance traces have been overlapped under the same series resistance of 25.2 Ohm).

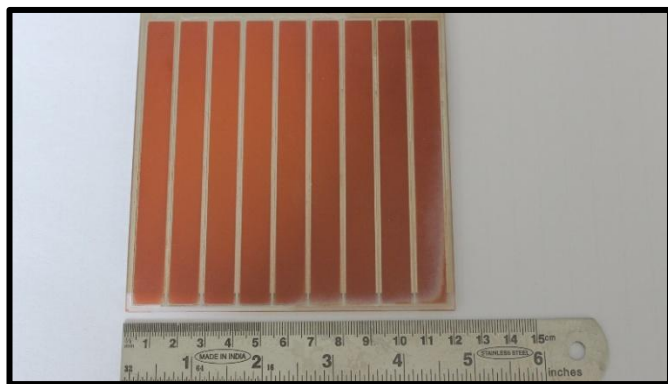


**Fig. 9.** A dye-sensitized solar module ( $12 \times 12 \text{ cm}^2$ ) fabricated at the optimized film thickness of  $12 \mu\text{m}$ .

$10^5 \text{ Hz}$  to  $0.005 \text{ Hz}$  with ac amplitude of  $12 \text{ mV}$ . Literature says that at higher potentials, impedance plots show three arcs, where the middle arc corresponds to the recombination resistance at the  $\text{TiO}_2/\text{dye}/\text{electrolyte}$  interface.<sup>13-15</sup>

The **Fig. 8b** shows Nyquist plots of DSCs with the different  $\text{TiO}_2$  film thicknesses. The width of the middle arc corresponds to recombination resistance at the interfacial region ( $\text{TiO}_2/\text{dye}/\text{electrolyte}$  interface). From the impedance plots, we can observe that the width of second semicircle is the largest for the  $12 \mu\text{m}$  thick DSC. But as the thickness is gradually increased, the recombination resistance decreased. The EIS studies in the literature also provide that  $10 - 12 \mu\text{m}$  is the optimum thickness for DSCs with spherical  $\text{TiO}_2$  particles.<sup>16-18</sup> Thus, from EIS studies; we can infer that  $12 \mu\text{m}$  thick film offers the minimum interfacial recombination in the device.

The  $12 \times 12 \text{ cm}^2$  DSC module (**Fig. 9**) with  $12 \mu\text{m}$  thick  $\text{TiO}_2$  film has shown an efficiency of  $3.28 \%$  (**Fig. 10**). The solar module consisted of 9 parallel rectangular compartments of  $111 \times 10.3 \text{ mm}$  dimension. It can be connected to an external circuit from the edges of the photoanode and the counter

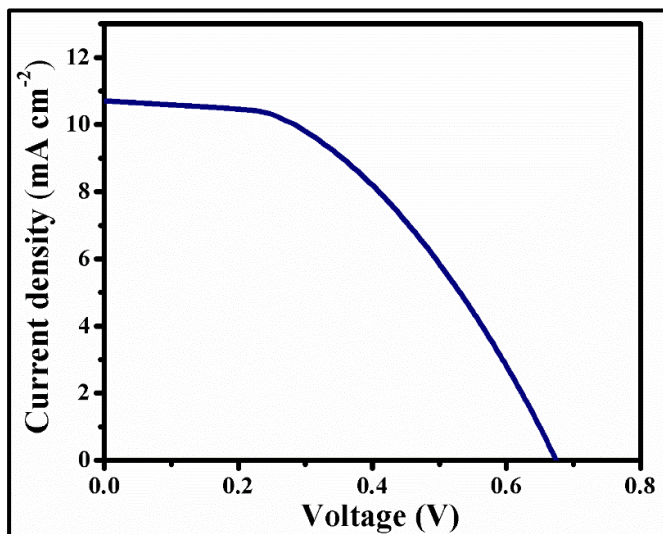


**Fig. 10.** Current density-Voltage (J-V) characteristics of the  $12 \times 12 \text{ cm}^2$  module.

electrode. The open-circuit voltage of  $0.674 \text{ V}$  was obtained for module with current density of  $10.71 \text{ mA cm}^{-2}$ . The fill-factor (%) of module was about  $45.4\%$ , which indicates power losses in the system due to series resistance. The resistance at Pt/electrolyte interface, TCO substrate resistance and diffusion resistance of  $\text{I}_3^-$  ions in electrolyte contribute to the series resistance in DSCs.<sup>19</sup> In the scaling up of DSCs, the contact area of TCO with the electrolyte and the amount of effective electrolyte are increased considerably which would contribute to increase of series resistance of the cell. This would essentially lower the FF and hence the efficiency.<sup>20</sup>

## Conclusions

We have adopted spray pyrolysis deposition technique as one of the simple and scalable approaches to fabricate thin films of the  $\text{TiO}_2$  for fabrication of DSC cells and module. The  $\text{TiO}_2$  thickness for best performing DSCs by spray pyrolysis deposition technique has been optimized as  $12 \mu\text{m}$ . At cell level (with  $0.2 \text{ cm}^2$  active area and thickness of  $12 \mu\text{m}$ ), a power conversion efficiency about  $7.79\%$  has been obtained. Using this optimized thickness, a  $12 \times 12 \text{ cm}^2$  DSC module has been created using the precise fabrication methods as outlined. The power conversion efficiency about  $3.28\%$  was obtained for the DSC module.

## Acknowledgements

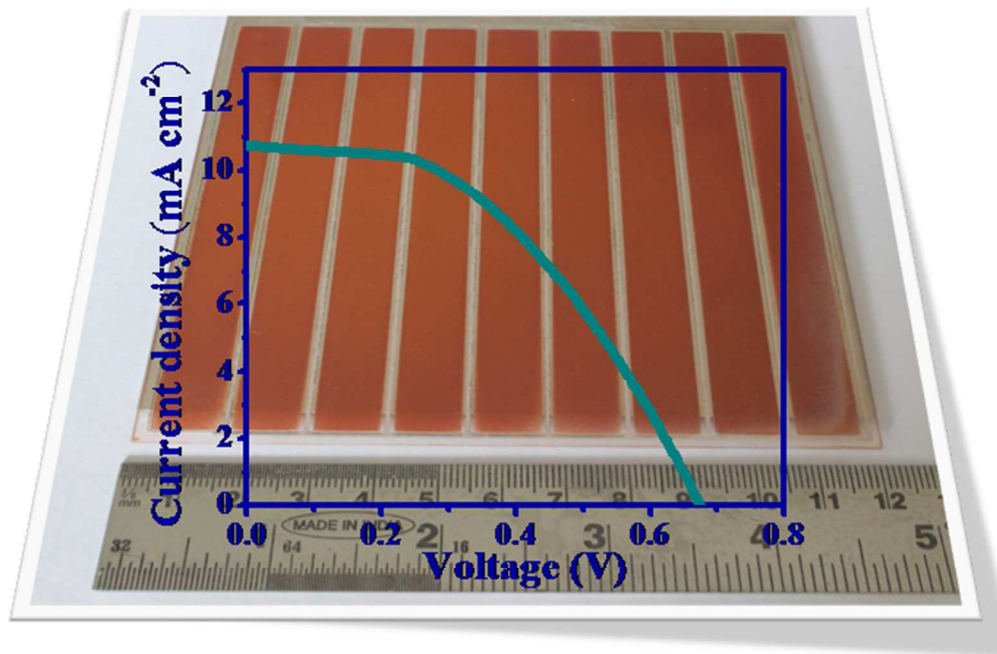
The authors thank the Ministry of New and Renewable Energy (MNRE) and Department of Science and Technology, Govt. of India for financial assistance.

## Notes and references

<sup>a\*</sup> Nanosolar Division, Amrita Centre for Nanosciences & Molecular Medicine, Amrita Institute of Medical Sciences, AIMS PO, Ponekkara, Kochi 682041, Kerala, India.

- (a) K. G. Reddy, T. G. Deepak, G. S. Anjusree, S. Thomas, S. Vadukumpully, K. R. V. Subramanian, S. V. Nair and A. S. Nair, *Phys. Chem. Chem. Phys.*, 2014, **16**, 6838. (b) P. V. Kamat, *J. Phys. Chem. C*, 2007, **111**, 2834-2860. (c) L. M. Gonçalves, V. d. Z. Bermudez, H. A. Ribeiro and A. M. Mendes, *Energy Environ. Sci.*, 2008, **1**, 655-667.
- P. D. Moskowitz and V. M. Fthenakis, *Sol. Cells*, 1990, **29**, 63.
- P. D. Moskowitz and V. M. Fthenakis, *Sol. Cells*, 1991, **31**, 513.
- B. O'Regan and M. Grätzel, *Nature*, 1991, **353**, 737.
- [http://www.fujikura.co.jp/eng/rd/gihou/backnumber/pages/\\_icsFiles/aieldfile/2013/05/23/42e\\_30.pdf](http://www.fujikura.co.jp/eng/rd/gihou/backnumber/pages/_icsFiles/aieldfile/2013/05/23/42e_30.pdf).
- J. Burschka, N. Pellet, S. J. Moon, R. Humphry-Baker, P. Gao, M. K. Nazeeruddin and M. Grätzel, *Nature*, 2013, **499**, 316.
- <http://www.swissphotonics.net/libraries.files/TobyMeyerSolaronix.pdf>
- C. J. Brabec, and J. R. Durrant, *MRS Bull.*, 2008, **33**, 670.
- M. Grätzel, *Inorg. Chem.*, 2005, **44**, 6841.
- G. R. A. Kumara, S. Kawasaki, P. V. V. Jayaweera, E. V. A. Premalal, and S. Kaneko, *Thin Solid Films*, 2012, **520**, 4119.
- H. C. Choi, Y. M. Jung, and S. B. Kim, *Vib. Spectrosc.*, 2005, **37**, 33.

12. Q. Wang, J. E. Moser, and M. Grätzel, *J. Phys. Chem. B*, 2005, **109**, 1494.
13. J. Bisquert, *J. Phys. Chem. B*, 2002, **106**, 325.
14. M. Adachi, M. Sakamoto, J. Jiu, Y. Ogata, and S. Isoda, *J. Phys. Chem. B*, 2006, **110**, 13872.
15. F. Fabregat-Santiago, J. Bisquert, E. Palomares, L. Otero, D. Kuang, S. M. Zakeeruddin and M. Grätzel, *J. Phys. Chem. C*, 2007, **111**, 6550.
16. V. Baglio, M. Girolamo, V. Antonucci, and A. S. Aricò, *Int. J. Electrochem. Sci.*, 2011, **6**, 3375.
17. C. -Y Huang, Y. -C Hsua, J. -G Chena, V. Suryanarayana, K. -M Leeb, and K. -C Ho, *Sol. Energy Mater. Sol. Cells*, 2006, **90**, 2391.
18. S. Ito, T. N. Murakami, P. Comte, P. Liska, C. Grätzel, M. K. Nazeeruddin and M. Grätzel, *Thin Solid Films*, 2008, **516**, 4613.
19. L. Han, N. Koide, Y. Chiba, A. Islam, R. Komiya, N. Fuke, A. Fukui, and R. Yamanaka, *Appl. Phys. Lett.*, 2005, **86**, 213501.
20. M. G. Kang, N. G. Park, Y. J. Park, K. S. Ryu, and S.H. Chang, *Sol. Energy Mater. Sol. Cells*, 2003, **75**, 475.



181x118mm (300 x 300 DPI)



The photovoltaic performance of a dye-sensitized solar cell module (12 cm × 12 cm) fabricated by spray pyrolysis deposition (SPD) of a TiO<sub>2</sub> colloid.